Rare Metal Materials and Engineering
Volume 50, Issue 6, June 2021
Available online at www.rmme.ac.cn

Science Press

Cite this article as: Wu Fan, Gan Guoyou, Yan Jikang, et al. Impact of SAL5356 and ER5356 Aluminum Alloy Welding Wires on Weld Structure and Joint Performance[J]. Rare Metal Materials and Engineering, 2021, 50(06): 1928-1934.

ARTICLE

Impact of SAL5356 and ER5356 Aluminum Alloy Welding Wires on Weld Structure and Joint Performance

Wu Fan[1], Gan Guoyou[1], Yan Jikang[1], Qiu Zhesheng[2], Wan Xiangming[3], Li Jiaqi[1], Zhang Bin[2], Yu Xianglei[1], Li Yanchao[1]

[1] Faculty of Material Science and Engineering, Kunming University of Science and Technology, Kunming 650093, China; [2] Yunnan Aluminum Co., Ltd, Kunming 650502, China; [3] Urban Institute, Kunming University of Science and Technology, Kunming 650093, China

Abstract: The wheel casting-extrusion method was employed to produce high-quality SAL5356 Al alloy welding wire, which was used to weld 6061-type Al alloy plates. The performance of SAL5356 welding wire was compared with that of the ER5356 welding wire by mechanical characterization, metallographic observation, microhardness and nanoindentation. The results reveal that under the same metal inertia gas (MIG) welding parameters, the SAL5356 welding wire endows superior tensile strength and yield strength to the weld joint, meeting the requirements of GB-2006-3880.2 standard (T general industrial aluminum and aluminum alloy plate and strip part 2: mechanical properties). Moreover, SAL5356 welding wire renders better stability than the ER5356 welding wire, which can be ascribed to the relaxed diameter and pitch of welding wire. Though further research is required to optimize the composition, microstructure and performance of SAL5356 welding wire, the current results demonstrate the potential of using local technology to produce 5356 Al alloy wire for high-end applications.

Key words: aluminum alloy welding; 5356 Al alloy welding wire; nanoindentation; metal inertia gas (MIG) welding

With the development of welding technology, Al and Al-based alloys have gained significant research attention owing to high strength, superior corrosion resistance and excellent welding performance[1-4]. Al-based alloys are widely employed in the transportation industry, such as high-speed rail, automobile and high-speed ship navigation[5-7]. One should note that modern transportation is characterized by high-speed, lightweight and safety. Therefore, welding technology plays a critical role in determining the performance of welded structure. Moreover, the quality of base material influences the welding process and quality of welded structure. For instance, 5356 aluminum welding wire is employed to obtain comprehensive properties of welded joints in large vehicles, subway and high-speed trains[8-12]. However, locally produced 5356 welding wire does not meet the strict industrial requirements, so high-quality 5356 welding wire of ER5356 was produced by Europe and the United States of America. Compared with the ER5356 welding wire, the locally produced welding wire renders inferior properties and poor surface quality[13-20]. The base material, welding mode, welding joint properties and microstructure of Al-Mg-Si series Al alloy have been extensively studied. Moreover, different problems of the welding process, such as porosity and softening of the welding joint, including softening of welding seam and softening of the base material, have been analyzed in detail and remedies have been proposed. However, a relatively fewer number of studies focused on 5XXX Al alloy joints, showing that the joint performance can be improved by controlling the phase structure, refining grain structure, and reducing defects and inclusions. In addition, the quality of welding joint can be improved by optimizing the process parameters and tuning the wire composition. Herein, the wheel casting-extrusion method is employed to prepare high-quality 5356 welding wire, and 6061 Al alloy plate, with a thickness of 15 mm, was welded by metal inertia gas (MIG) welding. The optimal welding parameters are determined, Moreover, the mechanical properties and microstructure of weld joints, realized by SAL5356 Al alloy wire and ER5356

Received date: June 03, 2020
Foundation item: Major Science and Technology Projects in Yunnan Province-Major Project of New Materials (2018ZE005, 2019ZE001)
Corresponding author: Gan Guoyou, Ph. D., Professor, Key Laboratory of Advanced Materials of Yunnan Province, Faculty of Material Science and Engineering, Kunming University of Science and Technology, Kunming 650093, P. R. China, E-mail: ganguoyou@kust.edu.cn

5356 Al alloy wire, were analyzed in detail.

1 Experiment

1.1 Welding process

Wheel casting-extrusion method was used to produce high-quality SAL5356 aluminum wire by Yunnan Aluminium Co., Ltd., China. Base material was 6061 aluminum alloy plate with dimension of 300 mm×150 mm×6 mm, single V groove of 45° and blunt edge of 2~3 mm were adopted. 99.99% Ar-shielded MIG welding was used in welding experiments.

Fig. 1 and Table 1 show the preparation process and the composition of SAL5356 and ER5356 welding wire, respectively. Preliminary experiments were carried out based on the dry elongation of 15 mm, gas flow rate of 20 L/min and plate spacing of 5 mm. The welding current of 200 A, wire feed speed of 12.4 m/min, filling layer current of 180 A, filling layer wire feed speed of 11.3 m/min, surface current of 150 A and surface wire feed speed of 9.4 m/min were used to weld. Both SAL5356 and ER5356 Al wires were used for welding and the welding process was carried out under the same conditions. The welding process can be divided into bedding, padding and covering, where the inter-pass temperature was set at 100 ℃. After each layer was welded, the surface was cleaned with a steel wheel to remove slag inclusions.

1.2 Characterization

The stability of welding wire was measured by the spatter degree of welding slag. The mechanical properties of welded joints were characterized by tensile and bending (forward and backward) tests using the WE-60 hydraulic universal material testing machine. The fracture morphology was observed by scanning electron microscopy (SEM, XL30ESEMTEP, Netherlands). The microstructure of welded joints was characterized by metallography (ZESS EVO18, Germany). The microhardness was assessed by a microhardness tester (HVST-1000, China). The hardness and elastic modulus were characterized by microhardness tester (Nanomechanics, Inc-inano, USA).

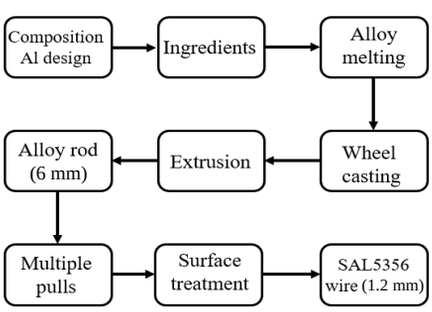

Fig.1 Preparation process of SAL5356 Al alloy welding wire

Table 1 Composition of 5356 welding wire

Wire-type	Si	Mg	Cu	Mn	Zn	Ti	Al
SAL5356	0.2	4.8	0.03	1.6	1.8	0.14	Bal.
ER5356	0.2	4.8	0.1	1.6	0.004	0.14	Bal.

2 Results and Discussion

2.1 Stability of welding wires

The spatter degree of welding slags under different welding current was analyzed to compare the difference in stability of SAL5356 and ER5356 welding wires. Herein, the quality of spatter particles is compared, as shown in Fig.2.

Fig.2 presents the influence of current on quality of welding spatter for both SAL5356 and ER5356 Al alloy welding wires, showing that the welding spatters grow with increasing the welding current. However, the growth trend of SAL5356 wire remains relatively flat, whereas the growth of ER5356 wire is significantly influenced by the high current. Overall, the total spatter mass of SAL5356 wire is smaller than that of the ER5356 wire, which indicates excellent stability of SAL5356 welding wire.

2.2 Fracture morphology

Fig. 3 shows the fracture morphologies of SAL5356 and ER5356 welding wires. It reveals an obvious dimple structure and ductile fracture under the action of tensile stress. Moreover, the SAL5356 welding wire exhibits obvious shrinkage, whereas the ER5356 welding wire does not demonstrate shrinkage, which can be ascribed to plastic deformation and stress concentration. In addition, large holes have been observed due to defects of welding wires.

2.3 Microstructure of weld metal

2.3.1 Preparation of metallographic samples

The metallographic samples were prepared by cutting 6061 T6 Al alloy after welding with both types of welding wires. The specimens were ground by sandpapers of 320#, 400#, 600#, 800#, 1000#, 1200# and 1500# to remove the surface scratches. Then, artificial corundum grinding paste was added in the polishing machine and specimens were corroded by 92 mL distilled water, and 6 mL nitric acid (1.4 and 20 mL of hydrofluoric (HF) acid 40%). The sample was corroded for 10 s and cleaned with alcohol, followed by drying. The optical microscope and ToupView software were used to capture the microstructural images, as shown in Fig.4.

Fig. 4 shows the microstructure of the parent material at

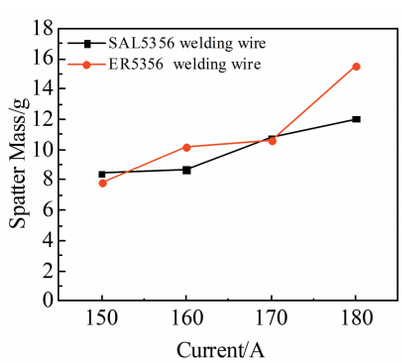

Fig.2 Spatter mass comparison between SAL5356 and ER5356 Al alloy welding wires

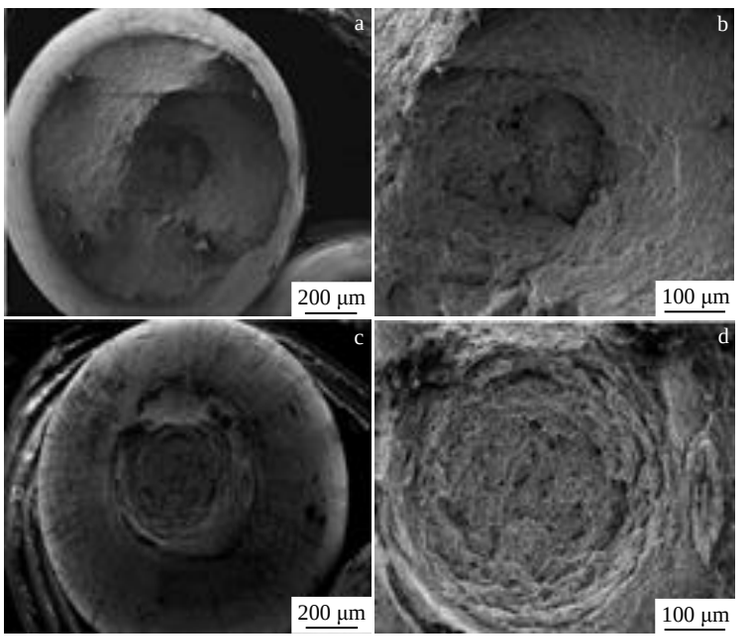

Fig.3 Fracture morphologies of SAL5356 (a, b) and ER5356 (c, d) welding wires

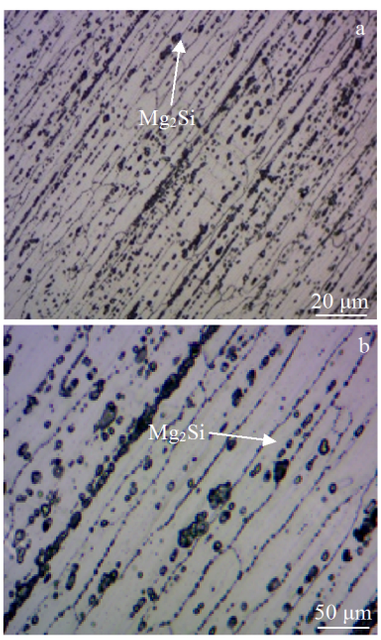

Fig.4 Parent material microstructures at magnifications of 200× (a) and 500× (b)

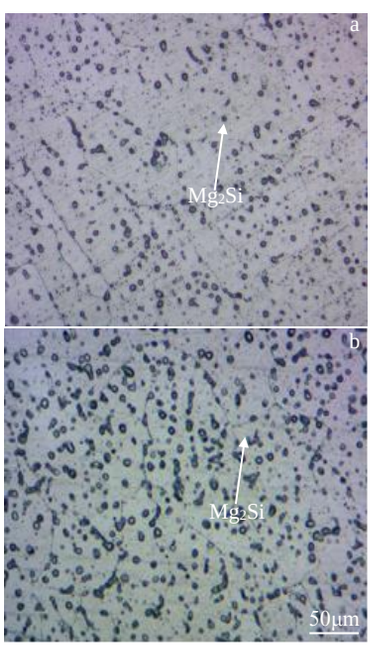

Fig.5 Microstructures of weld center: (a) SAL5356 welding wire and (b) ER5356 welding wire

200× and 500×, which clearly demonstrates that the 6061 T6 Al alloy possesses an obvious rolling direction and the deformation process does not alter the grain orientation. In digital micrographs, the high contrast represents the α Al substrate, whereas the low contrast represents uniformly dispersed β phase (Mg_2Si) particles.

2.3.2 Microstructure of welded joint

Fig.5 presents negligible difference between the microstructures of the weld centers, realized by SAL5356 and ER5356 welding wires. However, compared with the SAL5356 welding wire, the amount of secondary phase (Mg_2Si) particles is significantly increased after the application of ER5356 welding wire. In addition, the distribution of secondary phase (Mg_2Si) particles becomes more uniform.

Fig.6 shows the microstructure of heat-affected zones of the

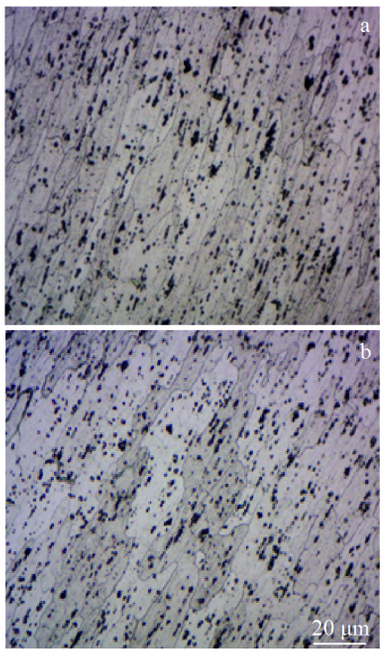

Fig.6 Microstructures of heat affected zone: (a) SAL5356 welding wire and (b) ER5356 welding wire

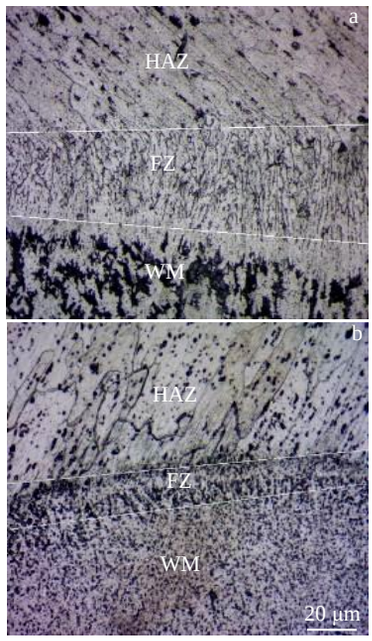

Fig.7 Microstructures of welded joint: (a) SAL5356 welding wire and (b) ER5356 welding wire

weld joints. The grain size in heat-affected zone is significantly larger than that of the base material and weld zone, which leads to inferior mechanical properties of the heat-affected zone.

Fig. 7 shows heat-affected zone (HAZ), fusion zone (FZ) and weld seam (WM) of both types of weld joints. The stratification of different zones can be readily observed and the microstructure of the heat-affected zone remains the same as the parent material. However, grain distribution and grain size of the heat-affected zone are different from those of the parent material due to the high welding temperature. Briefly, the grain size of HAZ is larger than that of the FZ and WM. The fusion zone exists between the weld transition and parent material. After heating, melting and solidification, the parent material exhibits solidified and dendritic crystal structure. Moreover, FZ is affected by the degree of supercooling and the orientation of the crystallites becomes parallel to the parent material after welding with the 5356 wire. The grain size of the weld seam can be clearly seen at a magnification of 200×. The grain size of weld seam zone is larger than that of the heat-affected zone and fusion zone. Briefly, the SAL5356 welding wire renders a two-times larger fusion zone than the ER5356 welding wire, which can be ascribed to the superior stability of the welding wire produced by wheel casting-extrusion method.

2.4 Tensile properties

Table 2 shows that the tensile strength of parent metal is 343.4 MPa, exceeding 17% of the 290 MPa found in the requirements of GB-2006-3880.2 standard (T general industrial aluminum and aluminum alloy plate and strip part 2: mechanical properties), which is because this part of material produces certain deformation strengthening after stretch straightening or roll straightening. Moreover, the tensile test specimen is sampled in the rolling direction of the material, which possesses higher mechanical properties than the standard. The fracture surface shows obvious necking, which can be ascribed to plastic deformation and stress concentration. Interestingly, the tensile and yield strength of SAL5356 wire are slightly higher than those of the ER5356 welding wire in Table 3, indicating that the SAL5356 welding wires can replace the ER5356 wires for high-end applications.

Table 2 Tensile data of the base material

Tensile strength/ MPa	Yield strength/ MPa	Elongation after breaking/%
343.7	293.5	16

2.5 Bending performance

The bending tests can be divided into positive bending and

Table 3 Tensile data of the welded joints

Material	Tensile strength/ MPa		Yield strength/ MPa		Fracture location
	Single value	Average value	Single value	Average value	
SAL5356 wire	239.6	236.2	169.6	182	HAZ
	232.8		194.3		HAZ
ER5356 wire	204.3	211	140.3	137	Fusion line
	216.8		133.7		Fusion line

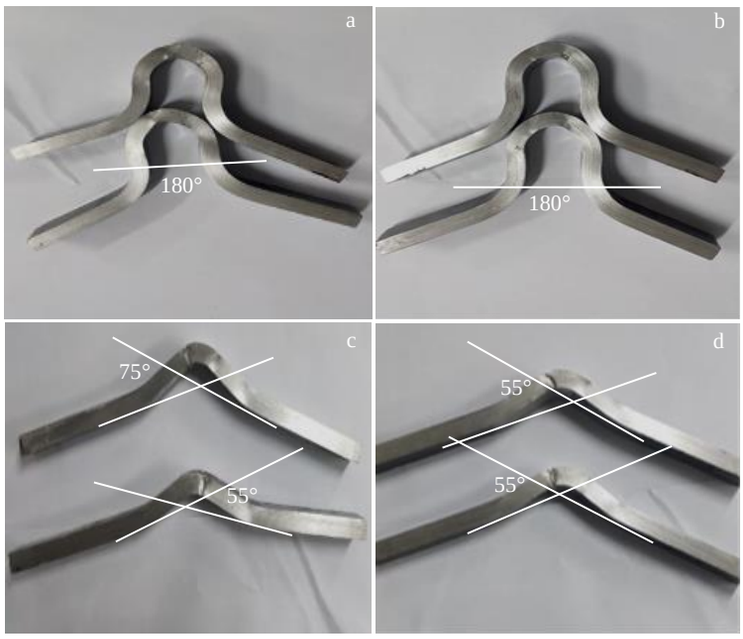

Fig.8 Back bending (a, b) and positive bending (c, d) specimens of SAL5356 (a, c) and ER5356 (b, d) welding wires

back bending, corresponding to the front and backside of the welded joint, respectively. It can be readily observed that the back bending angle of SAL5356 and ER5356 welding wire specimens reaches 180° without fracture and cracking, as seen in Fig. 8a and 8b. During the positive bending test, both SAL5356 and ER5356 wire samples broke. The highest and the lowest bending angles of the SAL5356 wire specimens are 75° and 55°, respectively, as seen in Fig. 8c, 8d. In addition, the ER5356 wire samples broke at a bending angle of 65°. Hence, both SAL5356 and ER5356 welding wires do not exhibit any significant difference in bending behavior.

2.6 Microhardness analysis

In order to demonstrate the hardness change in different zones, the microhardness was measured along a line, which is perpendicular to the symmetrical axis of the weld seam. The distance between two measurement points was 0.5 mm. The microhardness was measured in different zones, including base metal, heat affected zone, fusion zone and weld seam zone. The obtained results are presented in Fig.9.

Fig. 9 shows that the hardness distribution exhibits a W-shaped curve, showing that the hardness decreases from the weld seam zone to the fusion zone, followed by a gradual increase towards the heat-affected zone. Moreover, the hardness value initially decreases, and then rapidly increases close to the base material. One should note that the weld joint, realized by ER5356 welding wire, exhibits great fluctuations in the hardness data, whereas the hardness of weld joint, realized by the SAL5356 welding wire, remains stable from the fusion zone to heat-affected zone. Moreover, the hardness distribution in each area exhibits significant differences in the case of SAL5356 and ER5356 welding wires. In particular, the FZ width of the weld joints, realized by SAL5356 welding wire, is larger than that of the weld joints realized by ER5356 weld-ing wire, leading to significant differences in the hardness.

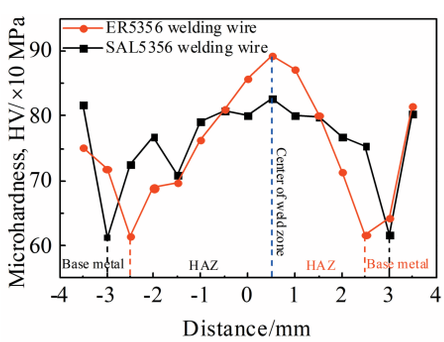

Fig.9 Microhardness distribution of welded joints realized by SAL5356 and ER5356 welding wires

2.7 Nanoindentation analysis

Fig. 10 shows the change in hardness of both types of weld joints from the weld seam zone to base material zone. The lowest hardness is exhibited by the HAZ2 region, which is consistent with the microhardness results. Moreover, the hardness value gradually decreases from the fusion zone to heat-affected zone, and then rapidly increases near the base material. The ER5356 welding wire renders larger fluctuations than the SAL5356 welding wire. The change in hardness can be ascribed to the microstructural transformation from the secondary phase β' (Mg_2Al_3) to β (Mg_2Si) phase. These observations are consistent with the microstructural analysis. The secondary phase particles, β' (Mg_2Al3), are precipitated in the center of the weld, whereas β (Mg_2Si) particles are precipitated in α-Al matrix in the base material. During this

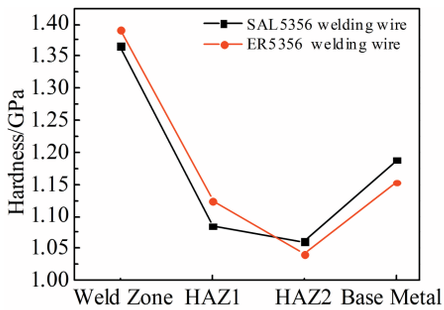

Fig.10 Change of hardness value from weld zone to base metal zone

process, the ER5356 welding wire forms the weld joint. One should note that a higher amount of β' (Mg_2Al_3) particles is uniformly precipitated in the center of the weld. Hence, the ER5356 welding wire endows higher hardness in the weld zone than the SAL5356 welding wire. Moreover, this explains the large fluctuations in hardness of weld joints realized by the ER5356 welding wire.

Fig.11 shows the elastic moduli of weld joints after welding with SAL5356 and ER5356 welding wires. The maximum elastic modulus is exhibited by the weld zone and it gradually decreases from the weld zone to base material, which can be ascribed to the difference in composition and microstructure of the weld zone and base material zone. Moreover, the plastic deformation during loading and unloading of the nanoindenter significantly influences the elastic moduli. Moreover, the welding process may induce residual stresses near the welding area, leading to a certain amount of strain. Abdel-Karim et al[21] have demonstrated the influence of residual strain on the elastic modulus of aluminum alloy. Therefore, the difference in elastic moduli of HAZ and base material can be attributed to the residual stress of heat-affected zone. Furthermore, the elastic modulus of weld joints realized by ER5356 welding wires remains higher than that of the weld joints obtained by SAL5356 welding wires. Hence, the ER5356 wires result in higher residual stress than SAL5356 wires. One should note that the presence of residual stress is considered as a welding

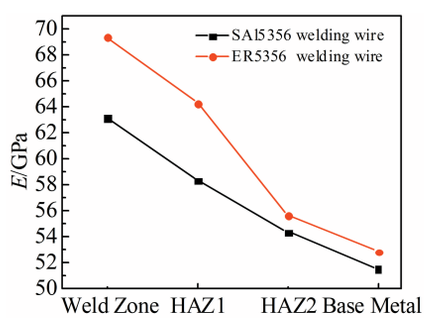

Fig.11 Elastic modulus of welded joints realized by SAL5356 and ER5356 welding wires

defect, so the performance of SAL5356 welding wire is better than that of the ER5356 welding wire.

3 Conclusions

1) The preliminary experiments reveal that the dry extension length of the welding wire is 15 mm, the mixed gas flow rate is 20 L/min and the welding plate clearance is 5 mm. Moreover, a series of experiments are conducted to determine the optimal welding parameters, including base layer, fill layer and cover layer parameters.

2) The total spatter mass of SAL5356 welding wires is not significantly different from that of the ER5356 welding wires. The un-melt wires can be observed in the spatter of ER5356 wires under low welding current, whereas the spatter of SAL5356 welding wires is much smaller than that of the ER5356 welding wires under high current.

3) The tensile data of base material meet the requirements of GB-2006-3880.2 standard (T general industrial aluminum and aluminum alloy plate and strip part 2: mechanical properties). The tensile strength of weld joints, realized by SAL5356 welding wires, reaches 80% of the tensile strength of the parent material. Moreover, the fracture occurs in the heat-affected zone, which implies that the weld joints meet the desired requirements for high-end applications. Moreover, the back bending reaches 180° without fracture or surface cracks. Owing to the softening of 6061 Al alloy weld joint, the heat-affected zone grains become coarser and microhardness decreases. In the case of SAL5356 wire, the fusion zone is larger than that of ER5356 welding wire. The microhardness of weld joints exhibits a W-shaped curve, i. e., the micro-hardness gradually decreases from the welding seam to the heat-affected zone, and then increases near the base material. The heat-affected zone exhibits minimum hardness due to the welding heat, corresponding to the weakest area of the weld joints.

4) Both SAL5356 and ER5356 welding wires exhibit similar quality and performance, and tensile strength, yield strength, welding stability, hardness and elastic modulus of SAL5356 welding wire are better than those of the ER5356 welding wire, while SAL5356 welding wire also contains certain defects. For instance, the welding process of SAL5356 welding wire is not stable under lower current, leading to the fried silk phenomenon. The mechanical characterization, microstructural analysis and microhardness measurements reveal negligible differences in the perfor-mance of SAL5356 and ER5356 welding wires. Further research is needed to enhance the stability of SAL5356 welding wire, and the current results present the potential of using local technology to produce high-quality ER5356 Al alloy welding wire.

References

1 Dixit M, Mishra R S, Sankaran K K. *Materials Science & Engineering A*[J], 2008, 478: 163

2 Yang C, Guo W, Zhang H *et al*. *International Journal of Electrochemical Science*[J], 2013, 8: 9308

3 Yang D, Li X, He D *et al*. *Materials & Design*[J], 2012, 40: 117
4 Sato Y, Arkom P, Kokawa H *et al*. *Materials Science and Engineering A*[J], 2008, 477: 250
5 Norman A F, Hyde K, Costello F *et al*. *Materials Science and Engineering A*[J], 2003, 354: 188
6 Suresh M, Sharma A, More A M *et al*. *Journal of Alloys and Compounds*[J], 2018, 740: 364
7 Boothmorrison C, Dunand D C, Seidman D N. *Acta Materialia* [J], 2011, 59: 7029
8 Mukhopadhyay A K, Kumar A, Raveendra S *et al*. *Scripta Materialia*[J], 2011, 64: 386
9 Van Dalen M E, Gyger T, Dunand D C *et al*. *Acta Materialia*[J], 2011, 59: 7615
10 Knipling K E, Seidman D N, Dunand D C. *Acta Materialia*[J], 2011, 59: 943
11 Liu Z, Li Z, Wang M. *Materials Science and Engineering A*[J], 2008, 483: 120
12 Singh V, Prasad K S, Gokhale A A. *Scripta Materialia*[J], 2004, 50: 903
13 Halevy I, Beeri O, Hu J. *Journal of Materials Science*[J], 2010, 45: 589
14 Fuller C B, Krause A, Dunand D C *et al*. *Materials Science and Engineering A*[J], 2002, 338: 8
15 Filatov Y A, Yelagin V I, Zakharov V V. *Materials Science and Engineering A*[J], 2000, 280: 97
16 Sawtell R R, Jensen C L. *Metallurgical and Materials Transactions A*[J], 1990, 21: 421
17 Lapasset G, Girard Y, Campagnac M H *et al*. *Materials Science Forum*[J], 2003, 426-432: 2987
18 Lee S, Utsunomiya A, Akamatsu H *et al*. *Acta Materialia*[J], 2002, 50: 553
19 Wen S, Xing Z B, Huang H *et al*. *Materials Science and Engineering A*[J], 2009, 516: 42
20 Wu Z, Song M, He Y H. *Materials Science and Engineering A* [J], 2009, 504: 183
21 Abdel-Karim M, Khan A. *International Journal of Plasticity*[J], 2010, 26(5): 758

SAL5356与ER5356铝合金焊丝对焊缝组织与焊接接头性能的影响

吴　凡[1]，甘国友[1]，严继康[1]，邱哲生[2]，万祥明[3]，李家奇[1]，张　斌[2]，余向磊[1]，厉彦超[1]
(1. 昆明理工大学 材料科学与工程学院，云南 昆明 650093)
(2. 云南铝业股份有限公司，云南 昆明 650502)
(3. 昆明理工大学 城市学院，云南 昆明 650093)

摘　要：比较了一种采用半连续铸造-挤压法制备的SAL5356铝合金焊丝与ER5356铝合金焊丝焊接接头常规拉伸力学性能、金相组织、显微硬度以及纳米压痕试验。结果表明，确定的惰性气体保护焊（MIG）焊接工艺参数下，SAL5356铝合金焊丝焊接接头的抗拉强度和屈服强度均优于ER5356铝合金焊丝。在电弧稳定性上，SAL5356铝合金焊丝在低电流时稳定性不如ER5356铝合金焊丝，而在高电流时SAL5356铝合金焊丝稳定性优于ER5356铝合金焊丝。并提出国产焊丝需要进一步提高质量稳定性。

关键词：铝合金焊接；5356铝合金焊丝；纳米压痕；MIG焊

作者简介：吴　凡，男，1996年生，硕士，昆明理工大学材料科学与工程学院，云南 昆明 650093，E-mail：1796189519@qq.com